Journal of Nuclear Materials 394 (2009) 1–8

Contents lists available at ScienceDirect

Journal of Nuclear Materials

journal homepage: www.elsevier.com/locate/jnucmat

Corrosion of high burn-up structured UO_2 fuel in presence of dissolved H_2

P. Fors [a,b], P. Carbol [b,*], S. Van Winckel [b], K. Spahiu [a]

[a] Chalmers University of Technology, Chemical and Biological Engineering, Nuclear Chemistry, 41296 Göteborg, Sweden
[b] European Commission, Joint Research Centre, Institute for Transuranium Elements, P.O. Box 2340, 76125 Karlsruhe, Germany

ARTICLE INFO

Article history:
Received 11 March 2009
Accepted 13 July 2009

Keywords:
HBS
High burn-up
Spent nuclear fuel
Corrosion
Irradiated
Reducing condition
Hydrogen
Groundwater

ABSTRACT

The influence of high burn-up structured material on UO_2 corrosion has been studied in an autoclave experiment. The experiment was conducted on spent fuel fragments with an average burn-up of 67 GWd/tHM. They were corroded in a simplified groundwater containing 33 mM dissolved H_2 for 502 days. All redox sensitive elements were reduced. The reduction continued until a steady-state concentration was reached in the leachate for U at 1.5×10^{-10} M and for Pu at 7×10^{-11} M. The instant release of Cs during the first 7 days was determined to 3.4% of the total inventory. However, the Cs release stopped after release of 3.5%. It was shown that the high burn-up structure did not enhance fuel corrosion.

1. Introduction

One of the major issues for nuclear reactor operators today is an extension of the authorized burn-up of LWR fuel. A high burn-up decreases the total mass flow in the fuel cycle and reduces the number of refuelling operations. Consequently, it leads to lower production costs and larger reactor availability [1–3]. The average discharge burn-up of LWR fuel assemblies has for this reason been increased in recent years from around 40 to 50–60 GWd/tHM [4].

Experiments have shown that UO_2 fuels with an average burn-up around or below 40 GWd/tHM have very limited release of matrix bound radionuclides to groundwater under bedrock repository conditions [5–11]. However, as the rim of the UO_2 fuel is re-structured into a high burn-up structure (HBS) when the local burn-up exceeds 60 GWd/tHM [1], the release of radionuclides might be significantly larger from high burn-up fuels than shown from previously studied fuels.

The HBS formation at the rim of a UO_2 fuel is a result of the Pu build-up owing to capturing of epithermal neutrons with energies matching absorption resonances in ^{238}U. This was first observed in the late 1950's [12]. The Pu content in the rim is more than twice as large as the average Pu amount in the fuel at an average burn-up of 60 GWd/tHM [13]. The consequence of this enrichment in fissile material is a local increase of the burn-up by approximately a factor of two [14]. This increase of local burn-up results in a modification of the fuel microstructure. The original UO_2 grains with a size of around 10 μm tend to subdivide into smaller grains of around 100–200 nm. This restructuring of the grains is associated with the formation of a local porosity that can reach up to 30% [13]. The restructured rim area is up to 200 μm thick [14]. For a fuel with an average burn-up of 60 GWd/tHM, the HBS corresponds to about 8% of the fuel volume.

The exact mechanism of the HBS formation is unknown; however, a number of theories have been suggested: (i) induction by radiation damage; (ii) polygonisation due to rare gas and metallic fission product accumulation; (iii) build-up of mechanical stress around fission bubbles; (iv) formation of micro-domains of overstructures giving planar defects [15]. Regardless of the mechanism, the formation of the HBS may be described by a number of consecutive phases: nucleation of re-crystallized grains, loss of xenon from the new grain structure, formation of micrometer size pores in the re-crystallized new structure, and growth of the new pores with increase in the local burn-up as they collect the gas from the surrounding re-crystallized grains [1].

As a result of the HBS formation, the protective UO_2 matrix, which has been shown able to retain the majority of the fission products from spreading with the groundwater in the repository [5–11], will be completely re-structured once the burn-up is increased. Both the smaller grain size of the HBS structure and the elevated dose rate, caused by increased actinide and fission product content, are expected to lead to an increase in the dissolution rate of the fuel. In view of the increase in discharge burn-up, corrosion data for spent high burn-up fuels under reducing conditions

* Corresponding author. Tel.: +49 7247 951 178; fax: +49 7247 951 591.
E-mail address: paul.carbol@ec.europa.eu (P. Carbol).

0022-3115/$ - see front matter © 2009 Elsevier B.V. All rights reserved.
doi:10.1016/j.jnucmat.2009.07.004

are, therefore, needed in order to complete the performance assessments for the final repositories [16].

This paper presents the results from a static corrosion study on HBS-containing fragments under conditions expected in a deep bedrock repository. The fragments, with an average burn-up of 67 GWd/tHM, were corroded for 500 days in a synthetic groundwater in presence of dissolved H_2. The results provide new information on the long term release of radionuclides from high burn-up structured material.

2. Materials and methods

2.1. Fuel

The high burn-up UO_2 fuel used for the study was irradiated for 1332 days in a commercial pressurized water reactor. The average burn-up of the fuel rod used for the experiment was calculated to 59.1 GWd/tHM. The irradiation proceeded under normal operating conditions, i.e., without power-ramping. Fuel data and irradiation history are given in Table 1.

A 10 mm long segment was cut from a position of the fuel rod exhibiting a flat burn-up profile, as observed by γ-scanning. The segment was core drilled to separate the fuel centre from its peripheral 725 μm thick part, see Fig. 1. Post-irradiation examination of the fuel identified a 100 μm thick high burn-up structure, see Fig. 2. The fuel containing the HBS material was detached from the Zircaloy cladding by use of external stress in a screw clamp. The de-cladded fuel fragments contained about 15 wt.% HBS. The millimetre-sized fragments were stored under dry N_2 atmosphere (<2 vol.% O_2) for one year before the start of the corrosion experiment.

A part of the core-drilled fuel was dissolved and the inventory of actinides and fission products was determined by ICP-MS. The Pu-vector and the ^{148}Nd-isotope were used as input for ORIGEN calculation [17], to obtain the complete fuel inventory. The specific activities of the main fission products and actinides are given in Table 2.

The ORIGEN calculation gave an average burn-up for the HBS-containing fraction to 67 GWd/tHM. Twenty fragments with a total mass of 0.26 g were selected and used in the corrosion experiment. The fuel surface to leachate volume ratio at the experiment start was approximately 0.2 m^{-1}. The α-dose rate from the fragments to a surrounding solution was calculated to approximately 0.5 Gy/s. No annealing or washing of the fuel was made prior to the corrosion experiment.

Table 1
Fuel and irradiation data of the rod [36].

Parameters	
Fuel data	
Fuel	UO_2
Fissile fractions	4.1 wt.% $^{235}U/U_{total}$
Fuel stoichiometry	2.0
Fuel density	10.4 kg/dm^3
Pellet diameter	9.13 mm
Pellet length	11 mm
Average grain size	10 μm
Fuel pin data	
Radial gap	0.085 mm
Fuel pin diameter	10.75 mm
Cladding thickness	0.725 mm
Cladding material	Zr-base alloy
Internal pre-pressure	22.5 bar (room temperature)
Irradiation data	
Total number of irradiation days	1332 effective fission power days
Number of irradiation cycles	4
Average linear power	250 kW/m
Average fuel burn-up	59.1 GWd/tHM

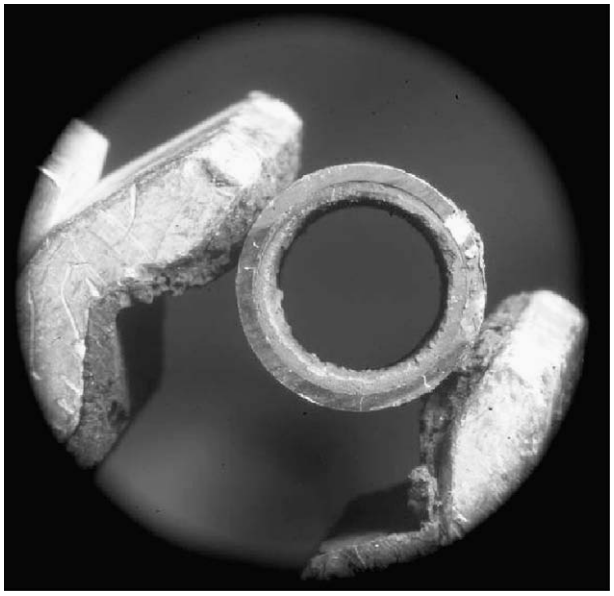

Fig. 1. The core-drilled fuel segment.

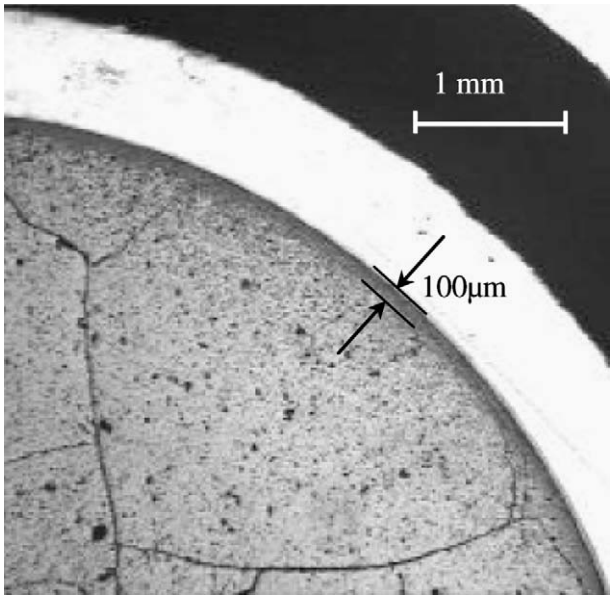

Fig. 2. Macro-photograph of the fuel showing the thickness of the high burn-up structure (HBS).

Table 2
Specific activities of the main fission products and actinides in the irradiated HBU fuel (rim containing fraction) as obtained by the ORIGEN calculation (as of 2008-07-07).

Fission products (Bq/g UO_2)		Actinides (Bq/g UO_2)			
^{90}Sr	4.1×10^9	^{234}U	3.8×10^4	^{241}Pu	4.9×10^9
^{125}Sb	7.8×10^7	^{235}U	2.2×10^2	^{242}Pu	2.1×10^1
^{134}Cs	1.2×10^9	^{236}U	1.4×10^4	^{241}Am	8.2×10^7
^{135}Cs	3.3×10^4	^{238}U	1.1×10^4	^{242m}Am	3.3×10^5
^{137}Cs	6.7×10^9	^{237}Np	2.6×10^4	^{243}Am	3.8×10^6
^{144}Ce	5.2×10^7	^{238}Pu	3.5×10^8	^{242}Cm	3.1×10^5
^{154}Eu	2.8×10^8	^{239}Pu	1.3×10^7	^{244}Cm	6.7×10^8
		^{240}Pu	2.6×10^7		

2.2. Leachant

Ultra pure mQ-water, >18 MΩ/m, (PureLab Ultra, Elga LabWater Ltd., UK) and suprapur grade chemicals (Merck GmbH, Germany)

were used throughout the experiment. The leachant contained 10 mM NaCl and 2 mM $NaHCO_3$. The composition has been chosen to mimic a low-saline granitic groundwater. The pH of the initial solution, 8.1, was measured with a combined pH-electrode (WTW SenTic Mic, and WTW pH340/ION analyser). The pH-electrode was calibrated with commercial pH standards (METTLER TOLEDO Inc., USA: pH 7.00 (Lot 1P039A), pH 9.21 (Lot 1N358B)). Cations as Ca^{2+} and Mg^{2+} have been excluded in the leachant to avoid the decrease of dissolution rates and/or potential formation of secondary uranyl phases [18–20].

2.3. Gases

The autoclaves were connected, by welded gas-lines, with a gas bottle. Two different gas compositions were used; pure H_2 (grade 6.0, Linde GmbH, Germany) and H_2/0.03% CO_2, (grade 5.6, Linde GmbH).

2.4. Autoclave and sampling

The corrosion experiment was carried out in a setup composed of two connected autoclaves (Parr Instruments Co., USA). The first autoclave, denoted experiment autoclave, was placed inside a hot cell, and had a volume of 620 cm^3. The second autoclave, denoted refill autoclave, was placed in a glove box. A welded stainless steal tube connected the two autoclaves. The refill autoclave could be equipped with either a 50 cm^3 or a 250 cm^3 vessel. The smaller pressure vessel was used during the start-up of the experiment and the larger in all actions thereafter. The hot cell and the glove box are both run under air atmosphere. A schematic drawing of the autoclave setup is shown in Fig. 3.

Both autoclaves were manufactured of quality grade II-weldable titanium, with a composition of 99.3 wt.% Ti, max. 0.3 wt.% Fe, max. 0.25 wt.% O, max. 0.1 wt.% C and the rest N and H. All wetted surfaces of the setup, i.e., pellet holder, magnetic stirrer, valves, security valves and tubings were made of titanium. Graphite gaskets and sealing-tape were used to avoid both metals, that exhibit a high sorption of actinides; and organic materials, which have poor radiation resistance. A welded tube without filters was used for solution transfer from the refill autoclave to the experiment autoclave. The dual-autoclave setup made it possible to refill, purge and sample solutions and gases without intrusion of O_2 into the autoclave. The entire setup was certified for H_2-pressures up to 6.5 MPa.

The leachate was sampled through a diving tube with an opening 8 mm above the bottom of the experiment autoclave. The overpressure in the autoclave was used to push leachate into 20-ml polyethylene (PE) sampling vials, inside the hot cell. The weight

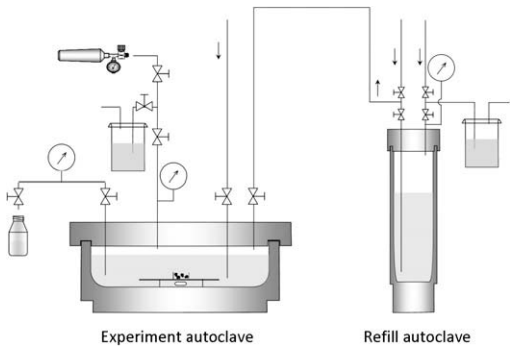

Fig. 3. Autoclave setup. The experiment autoclave in the hot cell is shown to the left, the refill autoclave located in a glove box connected to the experiment autoclave to the right. The setup has both solution and gas sampling possibilities.

Table 3
Elements selected for analysis by ICP-MS.

	Elements
Stable elements	Ti, V, Cr, Mn, Fe, Ni, Cu, Zn
Fission products	Rb, Sr, Zr, Mo, Tc, Ru, Ag, Cd, Sn, Te, Cs, Ba
Lanthanides	La, Ce, Pr, Nd, Sm, Eu, Gd, Tb, Dy
Actinides	U, Np, Pu, Am, Cm

of the sampled leachate was recorded for all samples. Subsequently, the leachates were transferred without filtration into 20-ml liquid scintillation counting vials (polypropylene) outside the hot cell. Analyses were made on aliquots taken from the LSC vial.

Leachates were sampled 13 times throughout the corrosion experiment; during filling (5 h after wetting the fuel), and after 1, 7, 62, 63, 138, 265, 313, 316, 319, 329, 442 and 502 days. The sampling sequence consisted of one rinse and two samples. The rinse served to collect all old, stagnant solution in the tubes leading from the reactor autoclave to the sampling outlet. The stagnant volume was estimated to ~5 cm^3, the volumes of the rinse samples ranged from 10 to 20 cm^3. The two (~10 cm^3) samples, taken after the rinse, were both considered as representative for the autoclave solution.

2.5. Analyses

Inductively coupled plasma mass spectrometry, ICP-MS (Thermo Element2, Thermo Electron Corporation, Germany), measurements were made on all samples to determine elemental concentrations of the elements shown in Table 3. Additionally, the concentrations of γ-emitters in the leachates were measured using a high-purity Ge-detector (EG&G Ortec Inc., USA). The concentration of hydrogen peroxide was determined by UV–vis light absorption spectroscopy and the Ghormley method [21]. The measurements were made on a USB2000 spectrometer (Ocean Optics Inc., USA). Further details regarding the ICP-MS and γ-spectrometry measurements are given in Ref. [22].

Gas mass spectrometry measurements (GSD 301 O2C OmniStar, Pfeiffer Vacuum GmbH, Germany) were carried out to identify all gases in the mass range 1–200 amu in the autoclave gas-phase, as well as to determine the concentration of N_2, O_2, CO_2, Kr and Xe. A three-point calibration with certified calibration gases (Linde/AGA GmbH, Germany) was made to obtain the response of the gas-MS (in cps) versus the gas concentration. Gas was collected from the autoclave into a 50 cm^3 stainless steel "gas-mouse" (SS-4CS-TW-50, Swagelok B.E.S.T. Fluidsysteme GmbH, Germany). After sampling, the gas mouse was removed from the autoclave and attached inside the hot cell to a welded gas transfer line equipped with particle filters. The other side of the transfer line was attached to the gas-MS, which was located outside the hot cell. Two measurements on the autoclave gas-phase were carried out; the first was made 12 days after the start of the experiment; the second was made after 313 days, i.e., directly before the washout action (see Section 3.3).

3. Experimental

3.1. Start-up

Prior to the start of the corrosion experiment and outside the hot cell, the autoclave was washed several times with mQ-water. Inside the hot cell, the fuel fragments were placed in a perforated titanium basket. A small Ti cylinder was placed on top of the fragments to stop them from leaving the perforated titanium basket. In order to avoid oxidation of the wet fuel surface by atmospheric

O_2, the autoclave was flushed with H_2 during, and for 15 min after the assembling of the leachant-free autoclave. The refill autoclave was used to transfer 38 cm^3 batches of leachant into the experiment autoclave. Before each of the 15 transfers, dissolved O_2 was physically displaced from the leachant by sparging it with H_2 for 15 min. The start leachant volume in the autoclave was 520 cm^3.

3.2. Experiment

The experiment was run for a period of 502 days without interruption. After the leachant filling, the autoclave was pressurized to 4.1 MPa with hydrogen. This pressure was kept throughout the experiment. The experiment was carried out at ambient hot cell temperature, 23 ± 4 °C. The leachate was not stirred.

The pH of the leachate after 5 h and after 1 day was measured to be 7.0 and 7.6, respectively. As the pH of the two leachates was lower than expected in a carbonate buffered leachant, 38 ml of a solution containing 10 mM NaCl and 30 mM $NaHCO_3$ was transferred on day 63. Measurement of the pH in the sample from day 63 (after the refill) gave 8.1.

The gas was changed from pure H_2 to H_2 + 0.03% CO_2 before the wash-out action on day 313.

3.3. Wash-out action

In order to lower the Cs concentration in the leachate, a wash-out action was carried out on days 313 and 314. The wash-out action consisted of seven stepwise dilutions of the stagnant 100 cm^3 leachate, which always remains below the diving tube in the autoclave after emptying. Batches of 216 cm^3 leachant were added to, and subsequently removed from, the autoclave giving a theoretical dilution in each step of 3.2. A break for the night was made before emptying the fourth refill leachate.

Each refill cycle lasted 40 min; however, most of this time was spent on sparging the refill leachant to remove dissolved O_2 before transfer to the experiment autoclave. The actual residence time in the experiment autoclave between solution transfer and draining was less than 5 min. After the wash-out, the autoclave was refilled and left with 500 cm^3 leachant.

4. Results

The corrosion experiment was carried out in presence of 4.1 MPa H_2, i.e., a dissolved H_2 concentration of 33 mM. All reported U, Pu and Tc values have been corrected for adsorption as described in Ref. [22].

4.1. Uranium and caesium

The measured concentrations of U and Cs are plotted as a function of corrosion time in Fig. 4. In addition, the deduced total amount of released Cs at the time for each sampling, i.e., the amount removed in samples plus the amount dissolved in the autoclave leachate, is shown (right hand scale) in the same figure.

The figure has been divided into three regions (top axis). Each break between two regions represents a change of the conditions in the autoclave. The first region shows the initial 62 days of the experiment, including the start-up. A decreasing U concentration is seen in the leachate throughout this region. Region 2 starts with addition of new HCO_3^- rich leachant into the autoclave on day 63 (see Section 3.2) and ends before the wash-out action on day 313. This region is characterized by decreasing U concentration and a stable concentration of Cs. The third region starts after a wash-out action on day 314 and lasts till the end of the experiment. In this region, a low and constant U concentration is seen together with a slow in-growth of Cs.

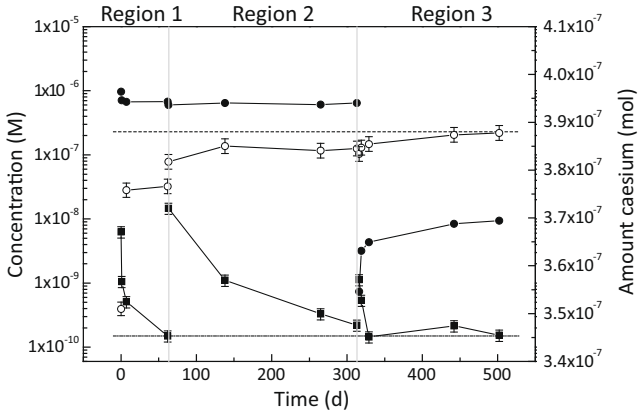

Fig. 4. Concentration of U (■) and Cs (●) on the left hand scale, and the amount of Cs (○) on the right hand scale, plotted as functions of corrosion time. The dash-dotted line shows a concentration of 1.5×10^{-10} M and the dashed line an amount of 3.88×10^{-7} mol. The error bars in the Cs concentration (±4%) are smaller than the data symbols. The uncertainty in the Cs amounts is ±6%; the main source to this uncertainty is the uncertainty of the calibration standard, while the mutual relative uncertainty between two values is in the range of ±0.4% (shown in the figure).

Region 1 shows a fast instant release of Cs from the fuel fragments and results in an instantaneous Cs concentration of 9.7×10^{-7} M in the first leachate. The subsequent leachates contain lower Cs concentrations as a result of additional filling of the autoclave (see Section 3.1). The amount of dissolved Cs remains constant at a level of 3.75×10^{-7} mol during the time period 7–62 days. On the other hand, the concentration of U in the leachate decreases by a factor of 40, from 6.3×10^{-9} M to 1.5×10^{-10} M, during the initial 62 days.

The sharp increase in the U concentration observed at the beginning of region 2 is a response to oxidation of the fuel surface. This can be deduced from the increased amount of dissolved Cs in the leachate. Oxygen must have intruded into the autoclave during the refill of the autoclave with 10 mM NaCl + 30 mM HCO_3^- leachant. The apparent lowering in Cs concentration between regions 1 and 2 is a result of the dilution caused by the solution transfer. After the initial increase and within the uncertainties of the measurements, the amount of Cs released stays constant for the remaining part of region 2. The U concentration decreases throughout region 2. It can be noted that it takes 250 days to get back to a concentration of 2×10^{-10} M.

Region 3 starts with a U concentration of 1×10^{-9} M in the first leachate, the same concentration as the last leachate collected during the wash-out action (see Section 4.4). Within 14 days, the U concentration decreased by one order of magnitude reaching 1.5×10^{-10} M. This U concentration remained stable until the end of the experiment. The concentration of Cs was lowered by three orders of magnitude during the wash-out action; but, as can be seen in region 3, it increases towards a new stable concentration at 1×10^{-8} M. The calculated release rate of Cs, after the wash-out action, is given in Table 4. It can be concluded that the

Table 4
Caesium release rate in region 3.

Time (d)	Δt (d)	Δn (mol)	$\Delta n/\Delta t$ (mol/d)
316–319	3	1.33×10^{-9}	4.4×10^{-10}
319–329	10	7.44×10^{-10}	7.4×10^{-11}
329–442	113	1.93×10^{-9}	1.7×10^{-11}
442–502	60	3.95×10^{-10}	6.6×10^{-12}

dissolution rate decreased two orders of magnitude during a time period of 186 days. At the end of the experiment, the total amount of Cs released from the fuel was calculated to 3.88×10^{-7} mol. This amount corresponds to 3.5 wt.% of the total Cs inventory in the fragments.

4.2. Neptunium, plutonium and technetium

The concentration of the redox sensitive elements Np, Pu and Tc is shown as a function of corrosion time in Fig. 5. The same regions are marked in Fig. 5 as previously discussed for Fig. 4.

Neptunium is, together with the other actinides, released at the beginning of the experiment due to dissolution of a pre-oxidized layer on the fuel surface. The well-correlated concentration decrease with the U seen during the first day of experiment indicates that Np is very probably co-precipitated with the U. After solution refills on day 63 and 313 the Np concentration increases above the detection limit (1×10^{-12} M). Most likely this Np originates from the previously precipitated U-phase, which becomes oxidized and dissolved by air oxygen that entered the autoclave together with the refill leachates. The Np/U ratio is close to the average inventory of the rim containing fraction in all samples with measurable Np concentrations, as seen in Table 5. This is probably due to the similarities between the Np(IV) and U(IV) ions, which make them co-precipitate as an ideal solid solution [23].

Owing to the dissolution of the pre-oxidized surface layer, also the Pu concentration shows a correlated increase with the U in the beginning of the experiment. After this initial increase, the almost parallel decrease in Pu and U concentrations indicate that also Pu is very probably co-precipitated with the U. During this co-precipitation part of the experiment, the Pu concentration passes through a minimum and then starts to increase towards a concentration of $\sim 7 \times 10^{-11}$ M. This level is reached at the end of all three regions and is marked in Fig. 5. In region 3, this increase in Pu concentration is especially apparent as it starts very low (due to the preceding wash-out action) is lowered even further in the first sample (due to co-precipitation), to thereafter increase towards 7×10^{-11} M at the end of the region. The Pu/U ratio at the end of each region is in the range between 0.24 and 0.50 (Table 5), i.e., far from the Pu/U ratio in the fuel of 0.015. This will be further discussed in Section 5.3.

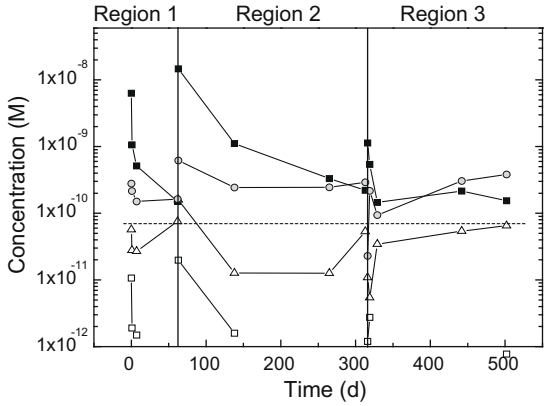

Fig. 5. Concentration of Np (□), U (■), Pu (Δ) and Tc (●) as a function of corrosion time. The dashed line marks a concentration of 7×10^{-11} M.

Throughout the first two regions of the experiment, the Tc is found at a relatively stable concentration range between 1×10^{-10} and 4×10^{-10} M. In the beginning of region 3, Tc had been removed during the wash-out action; however, the concentration increased again and the same level as before the wash-out was obtained at the end of the region.

A comparable Tc concentration of 4×10^{-10} M has been reported from a similar experiment on powdered spent fuel with a burn-up of 41.3 GWd/tU [6]. Since the low concentration show that the Tc is likely to be found in its reduced, Tc(IV) state, the concentration of Tc in solution is expected to be limited by the $TcO_2 \cdot nH_2O$/$Tc(OH)_2CO_3$(aq) equilibrium and reach 8×10^{-8} M [24]. This is clearly not the case, which indicates that also Tc may co-precipitate together with uranium, even though this precipitation is less apparent than for Np and Pu.

4.3. Lanthanides and americium

The concentration of La, Nd and Am is shown as a function of time in Fig. 6. The changes in concentration for the trivalent ions are well correlated (it becomes more apparent in the figure if the samples with concentrations at the detection limit are taken into account). As a result, changes in La concentration are expected to be representative for all trivalent ions in the system.

The concentrations of lanthanides and americium are much lower than the solubilities of their solid oxides or carbonates expected to form under such conditions, indicating an incongruent release from the fuel. A decrease in the Ln concentration is seen throughout the regions 1 and 2. This is likely to be caused by the reduction and precipitation of U, which co-precipitates Ln in order to form a solid solution in equilibrium with the leachate.

4.4. Wash-out action

The concentrations of Tc, Cs, U and Pu in the samples during the wash-out action are shown in Fig. 7. As a first step, the autoclave was drained (sample no. 1) so that 100 cm^3 leachate remained below the diving tube (see Sections 2.4 and 3.2). Batches of 216 cm^3 fresh leachant were transferred to the autoclave, and removed again, resulting in a theoretical dilution factor of 3.2 per transfer (sample no. 2–8).

From Fig. 7 it is seen that an oxidation and dissolution occurred during the first day (samples 2–4). The fuel oxidation occurred due to air intrusion into the gas line when the gas bottle was changed from H_2 to H_2/0.03 vol.% CO_2 (see Sections 2.3 and 3.2).

The oxidation of the fuel surface caused an increase in the concentration of the redox sensitive elements Tc, U and Pu. Oxidation

Table 5
Ratios between measured concentrations of Np, Pu, Am, Tc and Cs, and measured concentrations of U in leachates at the start and end of each region.

	In fuel	Region 1		Region 2		Region 3	
		Start	End	Start	End	Start	End
Np/U	9.2×10–4	1.7×10^{-3}	n.m.[a]	1.3×10^{-3}	n.m.[a]	1.1×10^{-3}	n.m.[a]
Pu/U	1.5×10^{-2}	9.0×10^{-3}	5.0×10^{-1}	1.1×10^{-2}	2.4×10^{-1}	9.7×10^{-3}	4.2×10^{-1}
Am/U	1.5×10^{-3}	3.5×10^{-4}	2.2×10^{-2}	2.6×10^{-4}	1.5×10^{-2}	n.m.[a]	1.3×10^{-2}
Tc/U	1.8×10^{-3}	4.4×10^{-2}	1.1	4.2×10^{-2}	1.3	2×10^{-2}	2.5
Cs/U	6.2×10^{-3}	1.5×10^{2}	4.5×10^{3}	4.1×10^{1}	2.9×10^{3}	6.5×10^{-1}	6.1×10^{1}

[a] Not measurable concentration.

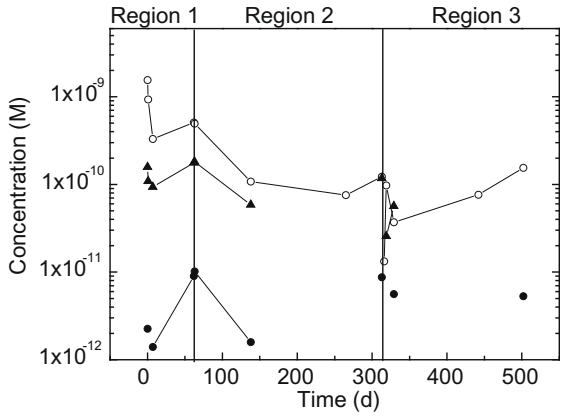

Fig. 6. Concentration in leachate of La (○), Nd (▲) and Am (●) as a function of time. Concentrations not shown are below the limit of detection for the ICP-MS, i.e., for lanthanides 1×10^{-11} M and for Am 1×10^{-12} M.

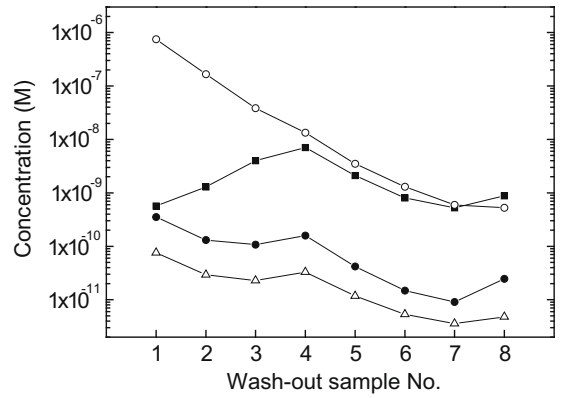

Fig. 7. Wash-out action after 313 days of corrosion; concentration in wash samples of Tc (●), Cs (○), U (■), and Pu (△).

of U appears to be strongly favoured in samples 1–4. This is verified in the third and fourth samples, which show a Pu/U ratio lower than the average fuel inventory. The Tc/U ratio in the leachate is never below the 1.8×10^{-3} found in the fuel (Table 5). However, since the co-precipitated phase is expected to be the more soluble than the pristine fuel, this phase will govern the ratio between new Tc and U release. From the concentration decrease in the beginning of regions 1 and 2 (Fig. 5), it is seen that the precipitating phase has a higher Tc inventory than the fuel average. Based on this and on the good correlation between Tc and Pu during the entire wash-out, U is probably the only element which is oxidized in the system. Technetium and Pu are probably released to the solution when the surrounding U atoms are dissolved.

The concentration of redox-insensitive Cs in the samples 2–7 is lowered by a factor of 3.1 in each wash, i.e., close to the expected dilution. This indicates that the oxidation seen in the first dilutions occurred on the precipitated U-phase. Nevertheless, due to the large amount of Cs in the first leachates a minor Cs release from pristine fuel could potentially have occurred without being detectable.

4.5. Gas measurement

The mass-spectrum (1–200 amu) from the gas collected on day 12 was identical to pure H_2 6.0. The concentration of both O_2 and N_2 was below the limit of detection (10 ppm) and no fission gases could be identified.

Table 6
Concentration and total amount of gases in the autoclave after 313 days of corrosion.

	Concentration (ppm)	Amount (mol)
N_2	1650	0.84
O_2	n.m.[a]	n.m.[a]
Kr	55	0.03
Xe	400	0.20

[a] Not measurable concentration.

The gas collected from the autoclave after 313 days of fuel corrosion contained except for H_2 only N_2 and small amounts of fission gases. The concentration and amount of N_2, O_2, Kr and Xe in the gas is given in Table 6. The concentration of 1650 ppm N_2 in the autoclave gas-phase is an evidence for air intrusion into the autoclave during the refill on day 63 (see Section 4.1). No O_2 could be detected despite the constant radiolysis and the air intrusion.

The ratio between the measured Kr and Xe concentrations is in good agreement with the expected cumulated fission yield for ^{235}U. The detection of fission gases in the autoclave gas-phase shows that previously closed fission gas bubbles in the fuel must have been opened at the fuel surface during the experiment, and that pristine fuel, thus, must have been dissolved. However, since the amount of each fission gas isotope was very low, no further conclusions could be drawn from the fission gas content.

4.6. Radiolytically produced H_2O_2

The theoretical production rate of oxidizing H_2O_2 in the system can be determined based on the calculated dose and tabulated [25] G-values (escape yields of radiolytically formed species as a function of the linear energy transfer of the emitted α-particles). This method of calculating the theoretical production rate of H_2O_2 yields 1×10^{-8} mol/day for our system.

Assuming that no H_2O_2 has reacted with the fuel matrix, the leachate is expected to contain 1×10^{-5} M H_2O_2 after 138 days of fuel–water contact. The spectroscopic determination of H_2O_2 in the leachate from day 138 gave a concentration below the practical detection limit of 1×10^{-6} M, which shows that the H_2O_2 had been consumed in the system.

5. Discussion

5.1. Effect of dissolved hydrogen on spent UO_2 fuels corrosion

A number of corrosion studies on UO_2 fuels with burn-ups lower than 43 GWd/tHM have shown that presence of more than 1 mM H_2 inhibits radiolytically induced UO_2 corrosion and keeps the dissolved U concentration at, or below, 10^{-8} M [5–7,10–11]. The long-term, stable, U concentration at 1.5×10^{-10} M observed in this work shows that 33 mM dissolved H_2 is enough to prevent radiolytically induced oxidative corrosion of UO_2 fuel fragments with an average burn-up of 67 GWd/tHM. Furthermore, as this fuel contained around 15 wt.% HBS with a local burn-up up to 120 GWd/tHM [14], it can be concluded that high burn-up structured material does not enhance fuel corrosion.

The gas sample from day 313 showed that 0.84 mol of atmospheric N_2 intruded the autoclave between day 63 and 313. A significant part of this probably entered as a spike during refilling on day 63 (see Section 4.5). In addition to the N_2, 0.23 mol atmospheric O_2 must have entered the system. However, no O_2 was detected during the gas mass measurement. Consequently, the system spent fuel–H_2–H_2O has the capacity to reduce not only the oxidative species formed through α-radiolysis, but also additional amounts of external oxygen. It should be noted that stable redox sensitive elements as Fe, Cr, Ni were present at

concentrations about 10^{-6} M in the solution. It is possible that e.g. Fe(II) in solution may have reacted with O_2 from air or radiolytic H_2O_2. The consumption of H_2O_2 in the bulk solution by the synergetic effect of Fe(II) ions and H_2 becomes then possible. Fe(II) ions react with peroxide via a Fenton type reaction:

$$Fe^{2+} + H_2O_2 = Fe^{3+} + OH^{\cdot} + OH^-$$

At the pH of our solutions Fe(III), precipitates as insoluble Fe(III)-oxide, but we do not notice a decrease in the Fe concentration. The hydroxyl radical produced from this reaction in an Ar atmosphere would oxidize another Fe^{2+} ion or U(IV), while in a hydrogen saturated solution the hydroxyl radical is expected to react very fast with molecular hydrogen to produce water and atomic hydrogen, which is a reducing radical:

$$OH^{\cdot} + H_2 = H_2O + H^{\cdot} \quad K = 4 \times 10^7\,\mathrm{L\,mol^{-1}\,s^{-1}}$$

This would explain also why Fe(III)-oxide precipitates, corresponding to the amounts of radiolytic H_2O_2 plus oxygen from air contamination were not observed in the autoclave.

During the start-up, an efficient dissolution of U(VI) from the pre-oxidized surface layer occurred due to the carbonates in the leachate. This led to an initial U concentration of approximately 1×10^{-8} M. The elevated U concentration decreased within a few days and ended, as mentioned above, at a level of 1.5×10^{-10} M. A nearly identical decrease in U concentration to a stable level of 1.5×10^{-10} M was observed by Ollila et al. in a similar system with un-irradiated UO_2 but with iron as reductant [10]. They interpreted this as a reduction of soluble U(VI) carbonates to less soluble U(IV). This interpretation has support in the NEA TDB [26], in which reduced U(IV) is found to be the only likely specie at such low solution concentrations. However, studies on U(VI) reduction from aqueous solutions have shown that once U(VI) is reduced, it precipitates as an amorphous $UO_2{\cdot}xH_2O$ phase with a solubility limit between $10^{-8.5}$ and $10^{-9.5}$ M [26–28]. Both the present study and the study by Ollila et al. [10] obtained lower dissolved U concentration. If the concentrations are assumed to be correctly measured, two possible explanations exist: (i) the previously measured and tabulated UO_2(am) solubility product is too high; or (ii) the precipitated U(IV) phase in the two experiments is more crystalline than the ones formed in previous studies. Further studies are required before a final conclusion can be drawn. However, since the experiments made to determine the solubility product of UO_2(am) have been carried out under rigorously controlled conditions and give repeatable results, explanation (i) seems unlikely.

Thermodynamic determination of the solubility product for a perfectly crystalline UO_2 solid at near neutral pH predicts solution concentrations down to 10^{-15} M [27,29,30]. If a more crystalline precipitate is formed in the present system, this could, therefore, explain the low solution concentrations. It is clear from the experiments by Parks and Pohl [28] that activated H_2 alone is not able to reproduce the low solution concentration seen in the present study. So even though the evidence is sparse, it is tempting to speculate an α-radiation induced hydrogen annealing, or crystallization process, in the amorphous precipitate. The authors strongly encourage studies to prove or discard this hypothesis.

5.2. Caesium release

The majority of the Cs in the leachate originates from an instant dissolution of the pre-oxidized fuel surface layer and from the Cs inventory immediately available at wetted grain boundaries. This can be concluded since 91% of the total Cs release was found in the solution already after 5 h.

The oxygen that inevitably entered the autoclave during start-up, led to a slow fuel surface oxidation and an additional Cs release during the first 7 days. The total Cs release during this first week measured to 97% of the overall release, see Fig. 4. The majority of the remaining 3% was released due to fuel surface oxidation after solution refill on day 63. In the first two regions of the experiment, no Cs release, and therefore no pristine fuel dissolution, could be assigned to the periods when the system was unaffected by external oxidants.

In the third region, the Cs concentration increases whereas the U concentration remains constant, see Fig. 4. This is, again, thought to be an effect of a slow fuel oxidation, which leads to Cs release due to exposure of new grain boundaries. The fuel oxidation was governed by air oxygen, which very probably entered the autoclave during the refill following the wash-out action. The low initial concentration of Cs made it possible to follow the fuel corrosion process. However, the amount of external oxidants in the system was limited and the release rate of Cs decreased with time, as can be seen in Table 4.

Interestingly, the uranium concentration remained stable near 1.5×10^{-10} M during the third region. This indicates the presence of a very efficient reduction of the oxidized and dissolved U.

5.3. Plutonium

In Section 4.2, the Pu release during the first day was described to originate from dissolution of a pre-oxidized fuel surface layer. The Pu in this layer might very well be oxidized to Pu(V). However, the concentrations of Pu in solution are always lower than 10^{-10} M, which indicates presence of Pu(IV) in solution [26]. From the tabulated redox potentials, the reduction of Pu(V) by U(IV) in acidic solutions is possible and given the similarities in actinide complexation the same should hold for the reduction of Pu(V) in our solutions by UO_2(s). It has been shown that UO_2(s) surfaces reduce Np(V) in solution [31].

As discussed above, all oxidized U atoms become reduced by the H_2 on the fuel surface. It is very probable that Pu(IV) oxide precipitates together with U(IV) oxide and forms a solid solution. The freshly precipitated solid solution phase will very probably govern the concentrations of U or Pu in the leachate [32].

As expected from the previous argumentation, the behaviour of U and Pu is well correlated in the first part of each region, see Fig. 5. However, at the end of the regions, the Pu concentration increases while U reaches a steady-state. This is not expected to occur in a system, where a solid solution is created by slow precipitation of dissolved species from the aqueous phase, since equilibrium is expected to be formed between the phases. The low U concentration at 1.5×10^{-10} M shows that reducing conditions prevail in the system. The increase in Pu concentration can, therefore, not be explained by a fuel surface oxidation. However, it is possible that a further reduction of the Pu(IV) to Pu(III) occurs on the surface. Such a reduction of Pu takes place if the Eh is below −300 mV (SHE) [33]. This would lead to an increased solution concentration of Pu due to the higher solubility of Pu(III) oxide [34] as compared to Pu(IV) oxide [35] and is tentatively proposed as a possible explanation.

5.4. Rate of U reduction

System-independent rate constants assuming zero-, first- and second-order reactions for the reduction rate were calculated based on the estimated fuel surface area (110 mm^2), and the U concentration together with solution volume at three stages of the experiment: (i) during region 1; (ii) during region 2; and (iii) the

beginning of region 3. Due to the high H_2 overpressure, an excess of H_2 is expected to be present near the surface. Hence, the reaction has been assumed to be independent of the dissolved H_2 concentration.

A slightly higher likelihood for a first order reaction was seen as compared to a zero-order reaction; however, both zero- and first-order reactions are held possible. The rate constant for the zero-order reaction was calculated to $k_{zero} = 10^{-15}$ mol/(m^2 s), and for the first-order reaction to $k_{first} = 10^{-6}$ m/s. The calculation excluded second order reaction. Zero-order reactions are typically found when a material required for the reaction to proceed, such as a surface or a catalyst, is saturated by the reactants, whereas first order reactions are expected if the reaction depends on the concentration of one reactant. In the studied system, both alternatives are plausible.

Interestingly, both k_{zero} and k_{first} show very good agreement with the rate constants recently calculated for a MOX fuel corroded under similar condition [22]. It can be speculated in whether the similar dose rate from the UO_2 fuel fragments in this work and the MOX fragments in [22] is the determining factor for the rate constants. Further experiments are needed to prove or disprove this observation. However, it is clear that analogous reduction behaviour is obtained in systems with two very different fuels. Consequently, it seems like the global fuel characteristics, such as surface area and dose rate, are more important for the reaction than any restructuring to HBS or inhomogeneity as Pu-agglomerate doping.

6. Conclusions

The results from our static corrosion experiment confirmed that 33 mM dissolved H_2 inhibits radiolytically induced UO_2 corrosion in the studied UO_2–H_2–H_2O system and that the high burn-up structure in the 59.1 GWd/tHM fuel did not enhance fuel dissolution.

Oxygen that entered the autoclave during refill did oxidize and dissolve the fuel resulting in U concentrations up to 2×10^{-8} M in the leachate. However, the dissolved U due to oxidation was repeatedly, reduced to a steady-state concentration of 1.5×10^{-10} M.

Uranium was shown to be released preferentially during oxidative dissolution of the matrix as compared to Pu.

The instant release of Cs was 3.4% during the first 7 days of the experiment. However, only 3.5% was released during the entire study. The results indicate that once the conditions in the system stabilize, the release of Cs decreases and probably at longer times than our test stops completely.

Redox sensitive Tc, Np, Pu and U are reduced in the system and co-precipitate onto the fuel surface, as shown in other studies [5]. External air oxygen seemed to preferentially oxidize U in this precipitated phase as compared to the pristine fuel surfaces.

Acknowledgements

We would like to thank V. Ernst, H.-M. Stutz and F. Blattmann in the design office and mechanical workshop. Many thanks to D. Baudot, D. Papaioannou, E. Toscano and J.-L. Arnoult for their help with the fuel. The hot cell team; E. Teixeira, M. Cardinale, A. Walschburger, B. Lynch and B. Christiansen are gratefully acknowledged. Further we would like to thank the operator of the nuclear power plant, for the allowance to use their high burn-up UO_2 fuel and AREVA NP for complementary fuel data. Thanks are also due to P. Peerani for performing the ORIGEN calculations. Finally the authors would like to thank J.-P. Glatz, D. Wegen and T. Gouder for reviewing the paper.

This work has partly been carried with support from the collaborative project RECOSY under the Seventh Framework Programme of the European Atomic Energy Community (EURATOM).

References

[1] J.-P. Hiernaut, T. Wiss, J.-Y. Colle, H. Thiele, C.T. Walker, W. Goll, R.J.M. Konings, J. Nucl. Mater. 377 (2008) 313–324.
[2] T. Sonoda, M. Kinoshita, I.L.F. Ray, T. Wiss, H. Thiele, D. Pellottiero, V.V. Rondinella, Hj. Matzke, Nucl. Instr. Meth. Phys. Res. B 191 (2002) 622–628.
[3] N. Lozano, L. Desgranges, D. Aymes, J.C. Niepce, J. Nucl. Mater. 257 (1998) 78–87.
[4] Y.-H. Koo, B.-H. Lee, J.-S. Cheon, D.-S. Sohn, J. Nucl. Mater. 295 (2001) 213–220.
[5] Y. Albinsson, A. Ödegaard-Jensen, V.M. Oversby, L.O. Werme, Mater. Res. Soc. Symp. Proc. 757 (2003) 407–413.
[6] K. Spahiu, L. Werme, U. Eklund, Radiochim. Acta 88 (2000) 507–511.
[7] K. Spahiu, D. Cui, M. Lundström, Radiochim. Acta 92 (2004) 625–629.
[8] A. Loida, B. Grambow, G. Karsten, P. Dressler, Mat. Res. Soc. Symp. Proc. 506 (1998) 923–924.
[9] A. Loida, V. Metz, B. Kienzler, H. Geckeis, J. Nucl. Mater. 346 (2005) 24–31.
[10] K. Ollila, Y. Albinsson, V.M. Oversby, M. Cowper, SKB Technical Report TR-03-13, Swedish Nuclear Fuel and Waste Management Co., Stockholm, 2003.
[11] S. Röllin, K. Spahiu, U.-B. Eklund, J. Nucl. Mater. 297 (2001) 231–243.
[12] D. Klein, W. Baer, G.G. Smith, Nucl. Sci. Eng. 3 (1958) 698.
[13] H. Bailly, D. Ménessier, C. Prunier, The Nuclear Fuel of Pressurized Water Reactor and Fast Neutron Reactors, Lavoisier Publishing, Paris, 1999. pp. 123–124.
[14] C.T. Walker, T. Kameyama, S. Kitajima, M. Kinoshita, J. Nucl. Mater. 188 (1992) 73–79.
[15] J. Noirot, L. Desgranges, J. Lamontagne, J. Nucl. Mater. 372 (2008) 318–339.
[16] L. Johnson, C. Ferry, C. Poinssot, P. Lovera, J. Nucl. Mater. 346 (2005) 56–65.
[17] O.W. Hermann, C.V. Parks, NUREG/CR-0200, Oak Ridge, September 1998.
[18] B.G. Santos, J.J. Noël, D.W. Shoesmith, J. Nucl. Mater. 350 (2006) 320–331.
[19] B.G. Santos, J.J. Noël, D.W. Shoesmith, Corros. Sci. 48 (2006) 3852–3868.
[20] C.N. Wilson, W.J. Gray, Mat. Res. Soc. Symp. Proc. 176 (1990) 489–498.
[21] C.J. Hochanadel, J. Phys. Chem. 56 (1952) 587–594.
[22] P. Carbol, P. Fors, S. Van Winckel, K. Spahiu, J. Nucl. Mater. 392 (2009) 45–54.
[23] D. Rai, N.J. Hess, M. Yui, A.R. Felmy, D.A. Moore, Radiochim. Acta 92 (2004) 527–535.
[24] T.E. Eriksen, P. Ndalamba, D. Cui, J. Bruno, M. Caceci, K. Spahiu, SKB Technical Report TR-93-18, Swedish Nuclear Fuel and Waste Management Co., Stockholm, 1993.
[25] B. Pastina, J.A. LaVerne, J. Phys. Chem. A 105 (2001) 9316–9322.
[26] R. Guillaumont, T. Fanghänel, J. Fuger, I. Grenthe, V. Neck, D.A. Palmer, M.H. Rand, Update on the Chemical Thermodynamics of Uranium, Neptunium Plutonium, Americium and Technetium, Elsevier Science Publishers, Amsterdam, 2003.
[27] D. Rai, M. Yui, D.A. Moore, J. Solut. Chem. 32 (2003) 1–17.
[28] G.A. Parks, D.C. Pohl, Cosmochim. Acta 52 (1988) 863–875.
[29] V. Neck, J.I. Kim, Radiochim. Acta 89 (2001) 1–16.
[30] K. Opel, S. Weiß, S. Hübener, H. Zänker, G. Bernhard, Radiochim. Acta 95 (2007) 143–149.
[31] Y. Albinsson, H. Nilsson, A.-M. Jakobsson, Mat. Res. Soc. Symp. Proc. 663 (2001) 1109–1115.
[32] D. Langmuir, Aqueous Environmental Geochemistry, Prentice Hall, New Jersey, 1997.
[33] P. Vitorge, H. Capdevila, S. Maillard, M.-H. Faure, T. Vercouter, J. Nucl. Sci. Technol. Suppl. 3 (2002) 713–716.
[34] A. Felmy, D. Rai, J. Schramke, J. Ryan, Radiochim. Acta 48 (1989) 29–35.
[35] V. Neck, M. Altmaier, T. Fanghänel, J. Alloy. Compd. 444–445 (2007) 464–469.
[36] Dr. Wolfgang Goll, Personal Communication, AREVA NP GmbH.